BEARING CAPACITY OF PRESTRESSED CONCRETE DECK SLABS

Amir, S., van der Veen, C., Walraven, J. C.
Department Design and Construction, Structural and Building Engineering, Concrete Structures, Faculty of Civil Engineering and Geosciences, Delft University of Technology, the Netherlands.

de Boer, A.
Ministry of Infrastructure and the Environment (Rijkswaterstaat), the Netherlands.

Abstract

In the Netherlands, most of the bridges were built more than 50 years ago and it is essential for designers to find out if these bridges are safe for modern traffic especially in shear since that was not considered in design recommendations before 1976. Detailed experiments have been carried out in the laboratory to investigate punching shear capacity of transversely prestressed concrete decks under concentrated loads. Various types of loading configurations were used and the effect of prestress level was studied. All the single load tests failed in punching of the deck slab and the slab-girder interface remained intact regardless of the position of the load. It was found that sufficient compressive membrane action (CMA) had developed in the deck slab due to lateral restraint and combined with the prestressing force, the bearing capacity was much higher than predicted by various codes and theoretical methods that do not consider the effect of CMA. This could lead to the conclusion that old bridges still have sufficient residual strength considering the beneficial effect of CMA.

Keywords: Deck slab, prestressing, concentrated loads, punching, compressive membrane action.

1 Introduction

There are around 69 bridges in the Netherlands with thin transversely prestressed decks cast in-situ between the flanges of precast girders that were constructed in the 60s or 70s of the last century. Since then traffic flow has increased making the safety of such bridges questionable according to the modern design codes. Also, the shear capacity as prescribed by the codes is more conservative in the recently implemented EN 1992-1-1:2005 (CEN 2005) than in the Dutch NEN 6720:1995. As a result, many existing bridges are found to be shear-critical when assessed using the Eurocode. Traditional methods of bridge design are based on conservative flexural theories and it has been discovered that under concentrated wheel loads, the deck slabs mostly fail in punching shear mode rather than flexural mode (Batchelor, 1990). Such behavior is attributed to the development of membrane forces in the deck slab. Compressive Membrane Action (CMA) or arching action occurs in laterally restrained slabs and provides enhanced bearing capacity in both flexure and punching shear. It is also logical that transverse prestressing of deck slabs will further enhance the capacity, so thinner deck slabs are possible with no problems of serviceability and structural safety. This paper describes the experimental research being conducted in the Stevin II laboratory, Faculty of Civil Engineering and Geosciences, Delft University of Technology, to investigate the capacity of a 1:2 scaled model of a bridge with a thin transversely prestressed concrete deck slab, cast between precast concrete girders) subjected to concentrated loads. Experiments are being carried out in order to investigate the effect of different parameters, like the transverse prestressing level (TPL), the geometry of the deck, the type of loading, on the punching shear strength. Until now 16 tests have been conducted and more are planned in future to further investigate this subject.

2 Experimental investigation

2.1 Real bridge

In a typical “approach” bridge, the deck slab is quite slender and is cast in-situ between the flanges of precast, prestressed concrete girders, Fig. 1.

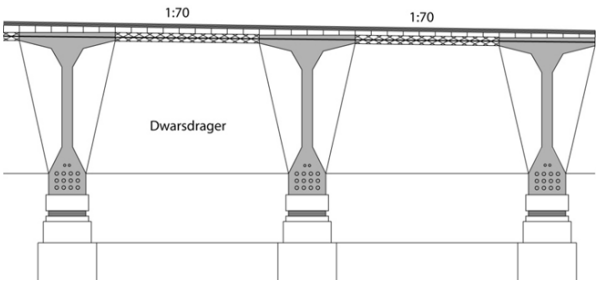


Fig. 1 Cross-section of bridge deck.

The transition of deck to flange is realised by an inclined indented interface. The interface between the slab and the girder is indented in order to generate sufficient shear capacity. The regular reinforcement ratio of the deck slab is quite low as prestressing reinforcement is already present. The prestressing tendons in the slab are placed in the transverse direction at an average spacing of around 650 mm c/c. In some places this spacing is 800 mm c/c. Transversely prestressed end transverse beams are present at the supports, along with diaphragms at 1/3 and 2/3 of the span. The bridge decks have been cast with a normal concrete strength, however, currently the concrete strength is considerably higher as a result of ongoing cement hydration during years.

2.2 Prototype of the bridge

In order to simulate an actual bridge as closely as possible, a 1:2 scale was used to design the prototype. The girders and the deck slab were designed in such a way that failure is expected to occur in the deck-slab as it is the slab which is the subject of interest in this research. To consider the most unfavourable effects in the investigation, the following lower bounds were considered during design.

- In a typical real bridge, the interface between the side of the upper flange of the girder and the cast in-situ deck is inclined to 5 degrees at one side of the deck slab but the prototype was provided with inclined interfaces at both sides.
- The spacing of the transverse reinforcement was increased from the general spacing of 650 mm c/c in the actual bridge to 800 mm c/c in the model.
- Most of the tests were done with a load applied in-between two adjacent transverse prestressing ducts in the deck. ***This gives a lower bound for the bearing capacity as compared to the capacity when testing directly above a prestressing duct.***
- Two transverse prestressing levels were applied: 1.25 MPa and 2.5 MPa. Although the usual TPL in a real bridge is 2.5 MPa, the value of 1.25 was applied to regard the eventual effect of tendon fracture. To adjust the prestressing level unbonded prestressed bars were applied.

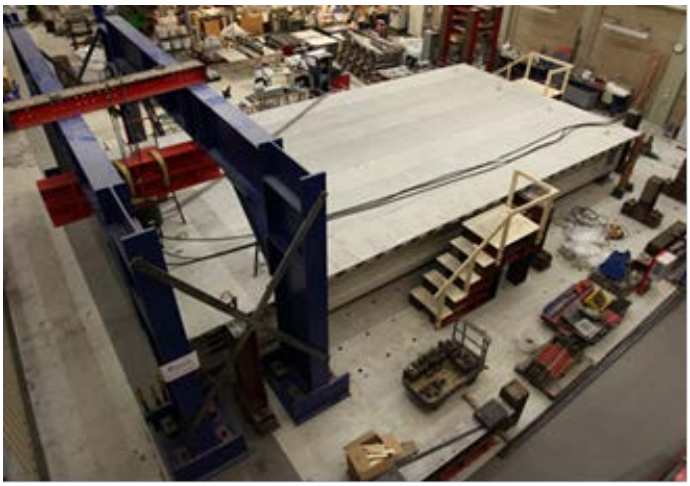


Fig. 2 Pictorial view of the test-setup in the laboratory.

2.2.1 General

The deck prototype was 12 m long and 6.4 m wide consisting of four precast concrete girders placed at 1800 mm c/c distance (Fig. 3). The deck slab was cast in-situ and post-tensioned in the transverse direction with a clear span of 1050 mm and a thickness of 100 mm. Two transverse beams were provided at the end of the girder-slab assembly, post-tensioned as well in the transverse direction (Fig. 3).

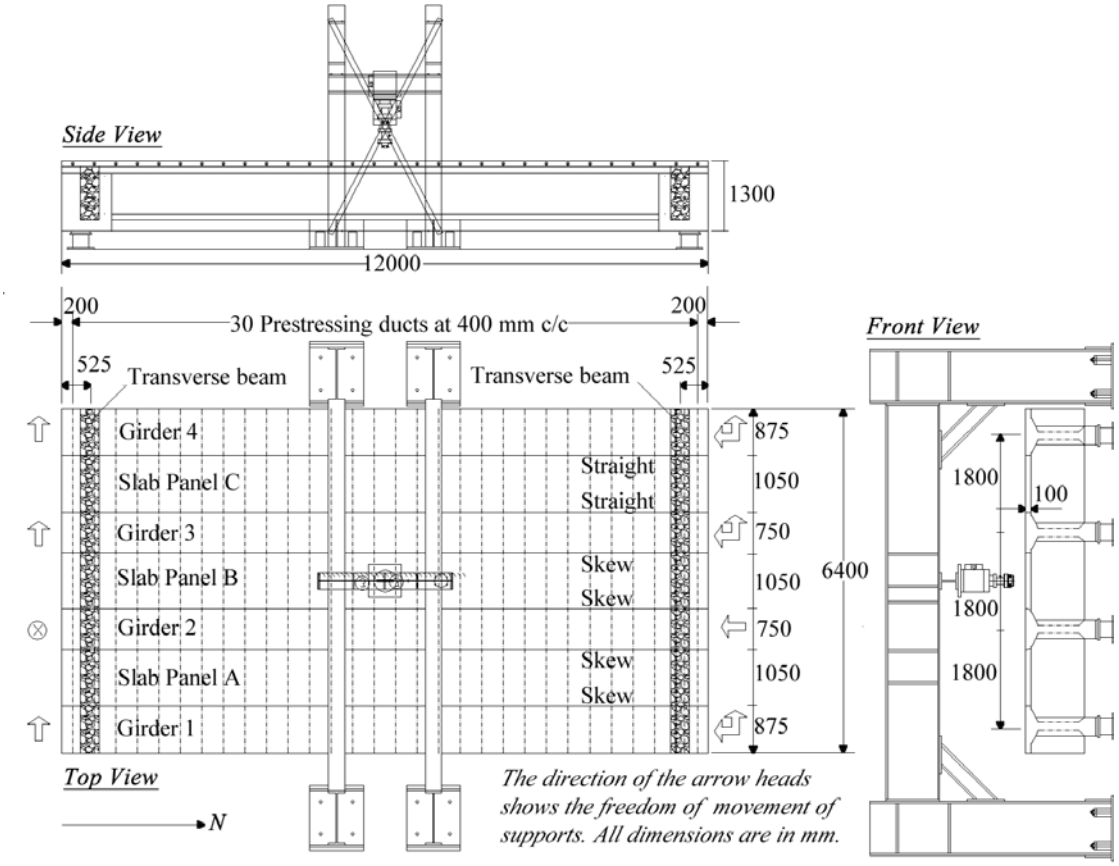


Fig. 3 Overview of the test-setup; Side view, Front view and Top view (clockwise from top).

2.2.2 Material properties

The material properties used in the deck slab panels are given in table 1. The concrete compressive cube strength and concrete tensile strength were found from the laboratory tests and the concrete cylinder strength and the modulus of elasticity was derived from EC2 formulas based on f_{cm}. The properties of the regular steel and the prestressing steel were taken from the relevant standard.

Table 1
Material properties of deck slab panels

Material	Units	Property	Value
Concrete	[MPa]	28 days Mean Compressive Cube Strength, $f_{cm,cube}$	75
		28 days Mean Compressive Cylinder Strength, f_{cm} ($0.8*f_{cm,cube}$)	60
		Mean value of Tensile Strength, f_{ctm}	5.41
		Modulus of Elasticity, E_{cm}	37659
Reinforcing Steel	[MPa]	Characteristic Yield Strength, f_{yk}	500
		Modulus of Elasticity, E_s (MPa)	200000
Prestressing Steel	[MPa]	Characteristic Tensile Strength, f_{pk}	1100
		Characteristic 0.1% proof stress, $f_{p0.1k}$	900
		Modulus of Elasticity, E_p	205000

2.2.3 Components of the test-setup

Four precast-prestressed girders were made by Spanbeton, the Netherlands and later transported to the laboratory. The cross section of the girders is as shown in Fig. 4. The exterior girders had an extended width of 125 mm at the exterior flanges to make sure that the prestressing and the confining effect was introduced adequately. Some of the interfaces between the deck slab panel and girder flange were inclined (1:20) and their location in plan is shown in Fig. 3 (top view).



Fig. 4a Girders in the laboratory.

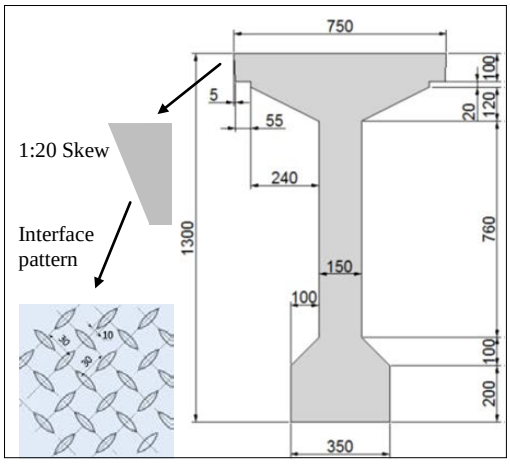


Fig. 4b Prestressed girder cross-section.

The support assembly for the girders consisted of 350 x 280 x 45 mm rubber bearing pads, 20 mm thick steel plates, a hinge and Teflon sheets. The interface between the slab and girder had an inclination of 1:20 with 1-2 mm deep, 30 x 10 mm long tear drop indentations (Fig. 4b), classified as smooth according to Eurocode 2.

The two transverse beams, 810 x 350 mm (Fig. 5), were cast at 525 mm from each end of the bridge deck (Fig. 3, top view). The top of the transverse beams was at 190 mm from the top of the girders. The beams were reinforced with Φ 8 mm stirrups at 250 mm c/c, and ten Φ12 mm bars in four layers in the longitudinal direction. The prestressing consisted of Φ15 mm bars in the transverse direction stressed to the same level as the deck slab.

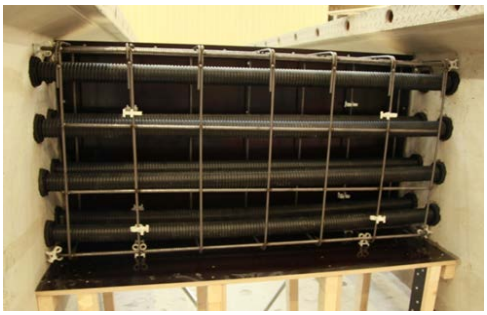


Fig. 5a Formwork and reinforcement for transverse beam.



Fig. 5b Prestressing bars for transverse beam.

In the deck slab, regular steel reinforcement was provided at both top and bottom with Φ 6 mm bars at 200 mm c/c in the longitudinal direction and Φ 6 mm bars at 250 mm c/c in the transverse direction. The transverse prestressing steel consisted of Φ15 mm unbonded bars post-tensioned to the desired level. The prestressing level was monitored to record any losses that could occur in time. Fig. 6 shows the deck slab ready for concrete casting.

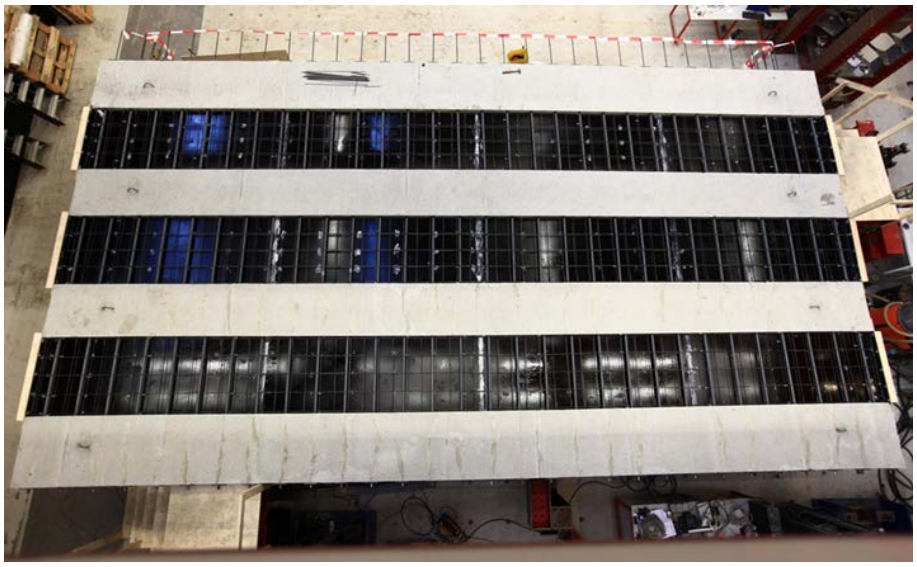


Fig. 6 Top view of deck slab. Ready for casting the deck slab panels.

2.2.4 Load Assembly and Instrumentation

Static tests were performed by using an electro-hydraulic actuator system. A concentrated load simulating a wheel print load was applied by the hydraulic actuator attached to an overhead reaction frame bolted to the floor Fig. 2. In all tests, the concentrated load was applied through a 200 x 200 mm, 8 mm thick rubber bonded to two 200 x 200 x 20 mm steel plates. The instrumentation is explained in Table 2.

Table 2
Instrumentation

Dimension	Units	Location	Instruments
Load	[kN]	Centre of the load	Load cell hydraulic actuator
Vertical deflections	[mm]	Midspan	Lasers/LVDTs around loading plate
		Supports	Lasers
		Girders	Lasers
		Slab-Girder joint	LVDTs across the loading position
Horizontal displacement	[mm]	Slab-Girder joint	LVDTs on top and bottom of slab panel
		Global deck slab	LVDTs/Lasers
Prestressing forces	[kN]	Slab/Cross beams	Load cells
Support reactions	[kN]	Girder supports	Load cells
Cracks	[mm]	Test location	Manual observation. Crack width card.

3 Testing program

To refer to the load configuration (according to Eurocode) and results of the test program the following abbreviations are used (Fig. 7):

- Point load acting at mid span of slab panel, P1M.
- Point load acting close to the girder flange-slab interface, P1S.
- Two point loads at 600 mm c/c acting at mid span of slab panel, P2M.
- Two point loads at 600 mm c/c acting close to the girder flange-slab interface, P2S.
- MSp = Midspan, ST= Straight joint, SK=Skewed joint, INT=Interface.

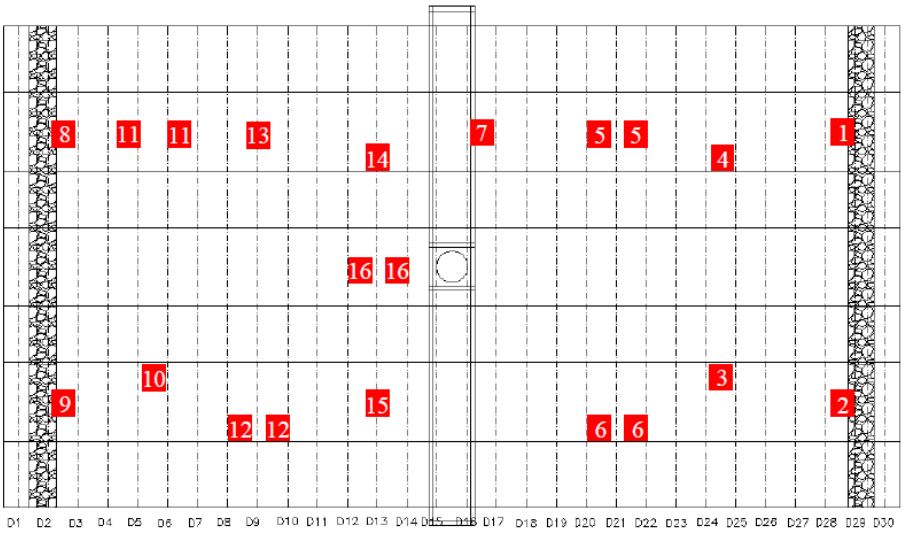


Fig. 7 Deck slab test positions highlighted. Duct positions labelled as D (#).

4 Experimental results

Sixteen tests have been performed until now. The main experimental results that will be discussed in this paper will be the ultimate/failure loads, the mode of failure, cracking load and cracking pattern. A summary of the test results is given in Table 3.

4.1 Ultimate loads

In this section two modes of failure are distinguished; Brittle Punching and Flexural Punching. Generally speaking, the governing mode of failure was brittle punching except when a double load was applied at midspan of the deck slab panel between two girders resulting in a flexural punching mode of failure. Most of the tests were performed in-between the prestressing ducts, hence the results represent a lower bound of the bearing capacity.

Table 3
Summary of Test Results

Test	Slab-Load Type	TPL	Joint	Initial hairline crack load	Cracking load (0.1 mm wide)	Failure load	Failure Mode
		[MPa]		[kN]	[kN]	[kN]	
BB1	C-P1M	2.5	ST	75	150	348.7	Brittle Punching
BB2	A-P1M	2.5	SK	75	150	321.4	Brittle Punching
BB3	A-P1S	2.5	SK	75	175	441.6	Brittle Punching
BB4	C-P1S	2.5	ST	100	175	472.3	Brittle Punching
BB5	C-P2M	2.5	ST	150	200	490.4	Flexural Punching
BB6	A-P2S	2.5	SK	150	250	576.8	Brittle Punching
BB7	C-P1M	2.5	ST	75	125	345.9	Brittle Punching
BB8	C-P1M	1.25	ST	50	100	284.5	Brittle Punching
BB9	A-P1M	1.25	SK	50	100	258.2	Brittle Punching
BB10	A-P1S	1.25	SK	25	100	340.3	Brittle Punching
BB11	C-P2M	1.25	ST	50	125	377.9	Flexural Punching
BB12	A-P2S	1.25	SK	100	175	373.7	Brittle Punching
BB13	C-P1M*	1.25	ST	25	75	322.9	Brittle Punching
BB14	A-P1S*	1.25	ST	25	125	295.9	Brittle Punching
BB15	A-P1M*	1.25	SK	50	125	359.7	Brittle Punching
BB16	B-P2M	2.5	SK	150	200	553.4	Flexural Punching

*Load was applied directly above a prestressing duct (Upper bound)

4.1.1 Brittle punching failure tests

When a single load was applied at midspan or when a single or double load was applied close to the support/interface, brittle punching failure was observed. The ultimate loads of brittle punching failure tests with regard to the type of loading, position of the load and the transverse prestressing level (TPL) are collected in Fig. 8. The three tests that were performed above the ducts are bounded black (Fig.8a). It can be seen clearly that an increase of the transverse prestressing level has a positive influence on the ultimate bearing capacity.

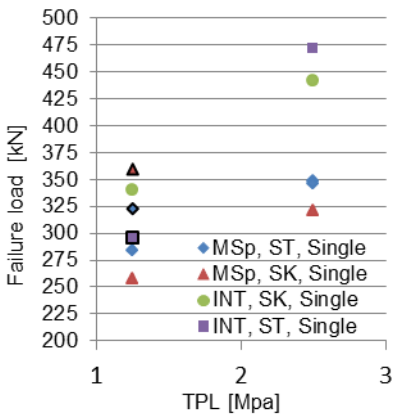


Fig. 8a Single load punching failure tests.

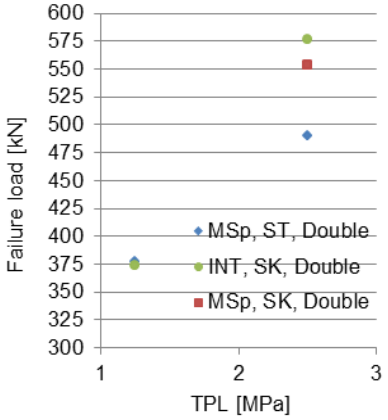


Fig. 8b Double load punching failure tests.

Fig. 9 shows the crack pattern observed in such tests. At punching failure the top side of the loading plate pushed through the slab resulting in a punching cone at the bottom side. In the double

load tests, one side punched through the slab first. Failure always occurred in the deck slab and the interface proved to have sufficient shear capacity whereas only some spalling occurred at failure.

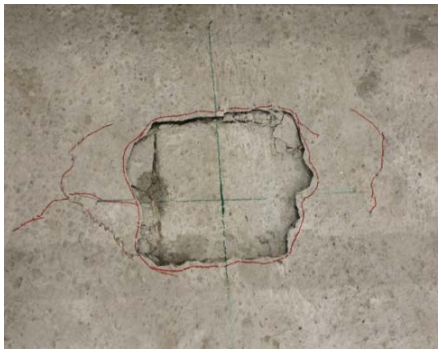


Fig. 9a Top side of the deck slab panel.



Fig. 9b Bottom side of the deck slab panel.

4.1.2 Flexural punching failure tests

Fig. 10 shows the ultimate loads and crack pattern of the double load applied at midspan. Large rotations occurred during loading and the longitudinal crack widened substantially approaching failure. However, the final failure still occurred according to the punching mode.

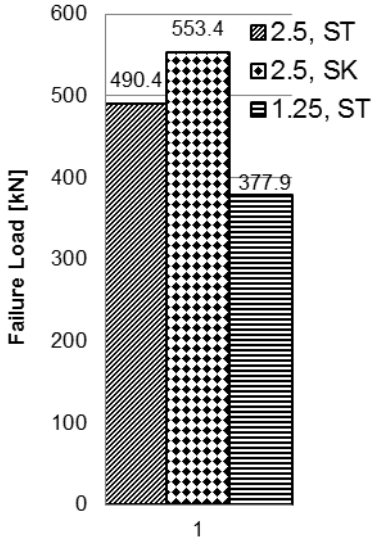


Fig. 10a Ultimate loads for double loads applied at midspan panel.

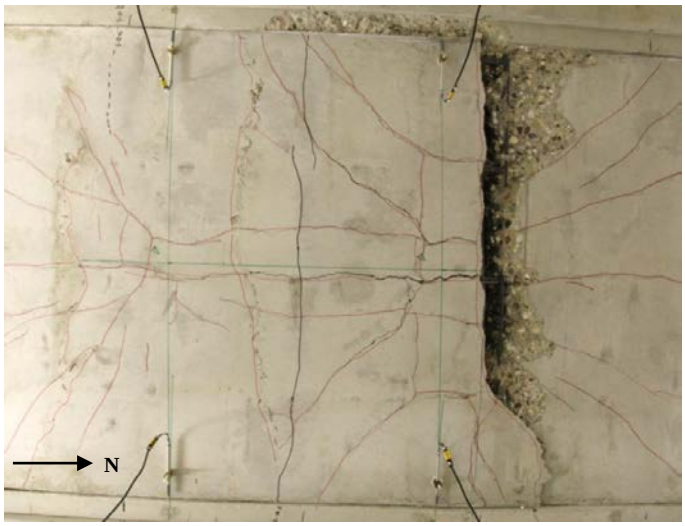


Fig. 10b Typical flexural punching failure mode.

4.2 Cracking pattern

For the tests with a single load applied at midspan and close to the support/interface, a punching cone was observed at failure as shown in Fig. 9. The initial cracks initiated directly under the loading plate at the bottom side of the deck slab. At higher load levels, radial/diagonal cracks were observed which propagated and widened further as the load increased. Circumferential cracks were observed close to failure but they were not always documented as observations were stopped, for safety reasons, close to the expected failure load.

For the double load tests carried out close to the joint/interface, a similar cracking pattern was observed but as expected, the cracks were clustered more towards the area of load application. A punching cone was observed at failure, however, no damage to the interface was observed except for some spalling of the bottom concrete cover of the flange at the failure stage.

For the double load tests conducted at the midspan of the deck slab panel, initial cracks were observed directly under the loading plate; subsequently a longitudinal crack joined the two loading points at the bottom side of the deck slab. As the load increased these cracks increased in width and radial cracking was initiated and also observed at both loading points. A significant increase was measured in the prestressing bars due to the large rotations occurring at midspan. Failure, however, finally occurred due to punching of one of the loading plates as shown in Fig. 10b.

The initial cracking load characterized by hairline cracks and the cracking load defined at 0.1 mm wide cracks (first significant cracks) are given in Table 3. As expected, a higher TPL delayed cracking and double loads and loads close to the support/interface showed higher cracking loads as compared to the single loads and loads at the midspan of the deck slab panel, respectively.

5 Results of calculation

5.1 Single load tests at midspan with failure in brittle punching shear mode

At present, codes like Eurocode 2 (2005) and ACI 318 (2005) do not consider CMA in their capacity formulae. However, there are some codes and methods that consider CMA for reinforced concrete only, like CHBDC (2005), the New Zealand (2003) code, UK BD81/02 (2002) and Park et al (1980). A comprehensive guide to compressive membrane action was given by Taylor et al (2002) outlining the research done at Queen's University Belfast.

Fig. 11a shows the punching shear capacity of single load tests with failure in brittle punching as calculated by the background report 25.5-02-37-prENV 1992-1-1(2002) (detail is given in section 5.1.1) and the ACI 318 (2005). No material factors have been used.

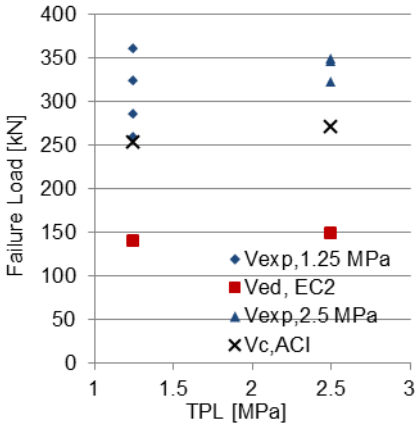


Fig. 11a Punching failure load predictions.

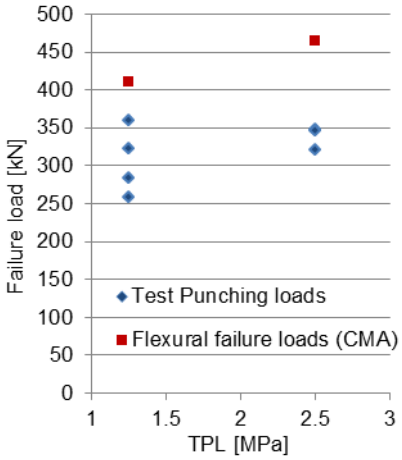


Fig. 11b Flexural failure load predictions.

The ACI 318 punching shear equation has a limitation on concrete strength which has been ignored and the actual slab concrete strength has been used. It can be observed that both codes underestimate the punching shear capacity. This lack of capacity is attributed to the ignorance of compressive membrane action.

The flexural capacity has also been calculated by a method developed by Park et al (1980) that considers CMA in reinforced concrete structures, and it can be seen from Fig. 11b that the experimental loads never reach the capacity in flexure. It can be concluded that although CMA enhances both punching shear and flexural capacity, it is the punching shear that becomes critical.

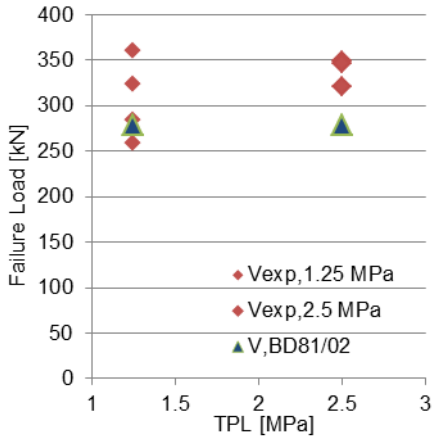


Fig. 12 Punching failure loads calculated by UK BD81/02 considering CMA.

Fig. 12 shows the punching failure capacity calculated by UK BD81/02 considering membrane action. It can be observed that ***the code predicts a conservative punching capacity probably because it was developed for reinforced concrete only.***

5.1.1 Background report 25.5-02-37 – prENV 1992-1-1:2002

The maximum punching shear capacity without compressive membrane action is calculated according to background report 25.5-02-37-prENV-1992-1-1:2002 for prestressed slabs (1).

$$v_{Rd,c} = C_{Rd,c} k (100 \rho_{ck})^{1/3} - k_1 \sigma_{cp} \qquad (1)$$

Where, $C_{Rd,c} = 0.18/\gamma_c$ ($\gamma_c = 1.0$) and $k_1 = 0.08$. The remaining parameters are the same as in EN 1992-1-1 (section 6.4.4).

According to the level II method (2), a reliable design equation can be derived with

$$B_{RD} = \mu_{BR} (1 - \alpha_{BR} \beta \delta_{BR}) \qquad (2)$$

Where, B_{RD} is the design value, μ_{BR} = mean ratio $V_{u,exp}/V_{u.calc}$ of test results, $\alpha_{BR} = 0.8$, $\beta = 3.8$ and δ_{BR} is the coefficient of variation of the tests results.

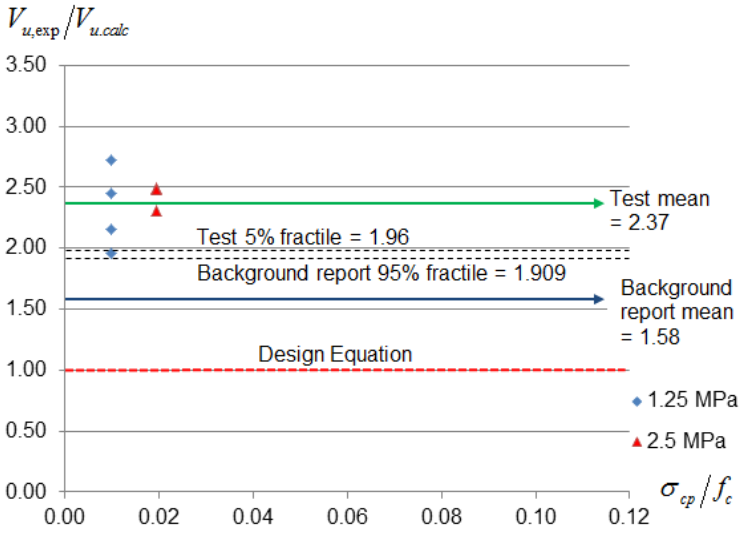


Fig. 13 Comparison of test results with punching shear equations according to the background report 25.5-02-37 – prENV 1992-1-1:2002 (Equations from EN 1992-1-1 recalculated to mean values).

The mean ratio $V_{u,exp}/V_{u.calc}$ (Fig. 13) for the tests is found to be 2.37 as compared to 1.58 given in the background report data and the 5% fractile of the tests is higher than the 95% fractile of the background report test data. Consequently, the increase in capacity is a result of compressive membrane action being developed during the experiments.

5.2 Double load tests with failure in the flexural punching shear mode

The flexural punching shear capacity considering CMA for double loads acting at midspan is calculated by assuming that the total flexural capacity is the sum of the arching moment capacity (Rankin and Long, 1997) and the bending moment capacity (BS5400). The effective width is calculated by the formula given by Taylor et al (2002). The formula is modified to incorporate two point loads acting at 600 mm c/c and the overlapping effective width due to loads being close to each other is corrected. Pucher charts (1964) have been used to find out the relationship between the moment and the load (moment factor). The method outlined by Taylor et al (2002) gives a fairly good estimation of the failure loads when compared to those observed in tests.

Table 4
Comparison of test and calculated capacity

Test	TPL	Test load	Predicted Flexural Punching load
	[MPa]	[kN]	[kN]
			Arching + Bending (Effective width = 1960 mm)
BB11	1.25	377.9	431.4
BB05	2.5	490.4	533
BB16	2.5	553.4	533

5 Conclusions

Ongoing experiments have shown that substantial CMA develops in the deck slab and transverse prestressing affects the bearing capacity positively. It was observed that failure always occurs in the deck slab span, regardless of the position of the load and the interface has proven to have sufficient strength and is never critical despite having an inclined surface. Also, **when loaded directly above a prestressing bar/duct, the deck slab shows a higher punching strength. Analysis of the current codes shows that the Eurocode 2 (2005) and ACI 318 (2005) have no provision for CMA and therefore underestimate this effect in the punching shear capacity formula**. Moreover, none of the code methods offers any provision to cope with compressive membrane action in prestressed slabs.

Acknowledgements

The authors would like to express their appreciation for Rijkswaterstaat, Ministry of Infrastructure and the Environment, the Netherlands, for supporting this research.

References

ACI Committee 318 (2005), Building Code Requirements for Structural Concrete (ACI 318-05) and Commentary (318R-05), American Concrete Institute, Farmington Hills, Mich.

Background report 25.5-02-37 – prENV 1992-1-1:2002, Section 6.4 (2002), J. C. Walraven, Delft University of Technology, the Netherlands.

Batchelor, B. de V (Routledge 1990), Membrane Enhancement in Top Slabs of Concrete Bridges, Concrete Bridge Engineering, Performance and advances, pp. 189-213.

BS5400: Parts 2 & 4, 'British Standard for the Design of Steel, Concrete and Composite Bridges', British Standards Institute, London (1978).

Canadian Standard Association: Canadian Highway Bridge Design Code (CHBDC), CAN/CSA-S6-00 (R2005), Canada.

ENV 1992-1-1:2005, Eurocode 2: Design of Concrete Structures – Part 1-1: General Rules and Rules for Buildings,.

NEN 6720:1995, Regulations for concrete: structural requirements and calculaton methods (in Dutch), Dutch Normalisation Institute (NEN).

Park, R.; Gamble, P. (1980), Reinforced Concrete Slabs, (John Wiley & Sons, UK).

Pucher, A. (1964), Influence surfaces of elastic plates, Wien, New York.

Rankin, G. I. B.; Long, A. E.(1997), Arching action strength enhancement in laterally restrained slab strips. Proceedings of the Institution of Civil Engineers, Structures and Buildings, Vol. 4, pp. 461 – 467.

Taylor, S. E.; Rankin, G. I. B.; Cleland, D. J. (2002), Guide to Compressive Membrane Action in Bridge Deck Slabs, Technical Paper 3, UK Concrete Bridge Development Group/British Cement Association.

Transit New Zealand Ararau Aotearoa (2003): New Zealand Bridge Manual, 2nd Edition.

UK Highways Agency, BD 81/02 (2002): Use of Compressive Membrane Action in bridge decks, Design Manual for Roads and Bridges, Vol. 3, Section 4, part 20, 20 pp.